Characterizing Phase Transitions in the Perovskites $PbTiO_3$ and $BaTiO_3$ Using Perturbed-Angular-Correlation Spectroscopy*

Gary L. Catchen, Edward F. Hollinger**, and Todd M. Rearick***

Department of Nuclear Engineering and Electronic Materials and Processing Research Laboratory, The Pennsylvania State University University Park, Pennsylvania 16802 USA

Z. Naturforsch. **51 a,** 411–421 (1996); received November 20, 1995

Perturbed-angular-correlation (PAC) spectroscopy was used to measure in ceramic samples of $PbTiO_3$ and $BaTiO_3$ the temperature dependence of the Ti-site electric-field gradients (EFGs) at temperatures very close to the ferroelectric-to-paraelectric transition temperatures T_c. The samples were doped with small amounts of Hf that carried the $^{181}Hf \rightarrow {}^{181}Ta$ probe radioactivity. A high-frequency nuclear quadrupole interaction that decreases very little as the temperature approaches T_c, characterizes the $PbTiO_3$ transition. The tetragonal and cubic phases for $PbTiO_3$ appear to coexist over a temperature interval of 8 ± 1 K, and the transition shows a thermal hysteresis of about 4 K. In contrast, a lower-frequency interaction that decreases rapidly as temperature approaches T_c, characterizes the $BaTiO_3$ transition. Both phases of $BaTiO_3$ appear to coexist over an interval of about 2 K, and the thermal hysteresis is about 1 K. At temperatures above T_c, both $PbTiO_3$ and $BaTiO_3$ show weak, non-vanishing Ti-site EFGs. Although, for $BaTiO_3$, this effect limits the accuracy with which critical effects can be measured, we estimate a power-law exponent $\beta = 0.21 \pm 0.05$, which most likely is somewhat lower in magnitude than the actual critical exponent. For the explanation of our observations we assume the existence of a distribution of T_c-values. This distribution would arise because the crystals could have spatially non-uniform distributions of nucleation sites, which for $PbTiO_3$ and $BaTiO_3$ could be point defects.

Key words: Ferroelectric, perovskite, nuclear electric-quadrupole, perturbed-angular-correlations, phase transition.

I. Introduction

During the past decades electric- and magnetic-ordering phase transitions, that occur in metal-oxide perovskite and related crystals, have been investigated. To characterize these transitions, macroscopic quantities such as heat capacities, electric and magnetic susceptibilities [1], and neutron[2] and x-ray [3] diffraction-derived parameters have been measured. However, by their very nature these quantities represent gross averages over the atomic-scale properties of these crystals. To measure the atomic-scale properties directly, spectroscopy has been applied.

To investigate ferroelectric transitions, Raman scattering has been used [4]. More recently, impulsive-stimulated Raman scattering [5] has been developed to provide more information about soft and heavily-damped vibrational modes that conventional frequency-resolved Raman scattering is not very sensitive to. But, because crystal vibrations represent collective motions that extend over the entire crystal, these light-scattering techniques do not provide detailed information about the effects of local fields that occur at specific lattice sites in a crystal. However, in electrically-ordered crystals, the effects of local crystal fields can provide important, unique information that can be used to distinguish, for example, between displacive and order-disorder mechanisms of ferroelectric transitions [6]. In magnetically-ordered crystals, the crystal-field information can provide, e. g., detailed information about antiferromagnetic transitions [7].

To investigate the effects of crystal fields, spectroscopic techniques that measure hyperfine inter-

---

* Presented at the XIIIth International Symposium on Nuclear Quadrupole Interactions, Providence, Rhode Island, USA, July 23-28, 1995.

** Current Address: Medical Physics Program, Rush University, Chicago, IL.

*** Current Address: Naval Undersea Warefare Center, New London, CT.

Reprint requests to Prof. G. L. Catchen.

0932-0784 / 96 / 0500-0411 $ 06.00

actions have been used, mostly perturbed-angular-correlation (PAC) [8] and Mössbauer-effect (ME) spectroscopies. Primarily magnetically-ordered perovskites have been investigated using ^{57}Fe [9] and ^{99}Ru [10] ME spectroscopy, but several non-magnetic, ferroelectric perovskites have also been investigated [11]. Studies of magnetic crystals have focused on characterizing exchange interactions [10] and measuring critical phenomena [9].

The PAC technique involves substituting a small number of radioactive probe ions into a specific site in the crystal of interest and measuring the hyperfine interaction at that site [8]. In non-magnetic crystals one measures the nuclear electric-quadrupole interaction and in cubic magnetic crystals the magnetic-dipole interaction. In lower-symmetry magnetic crystals one measures the combined nuclear magnetic-dipole and nuclear electric-quadrupole interaction [12]. During the measurement, the radioactive probe undergoes beta decay and populates an excited level in the daughter nucleus. This excited level decays by successively emitting two γ-rays. The first γ-ray populates an intermediate quantum level that has a long lifetime, and the second γ-ray depopulates this level. During the lifetime of the intermediate quantum level, the nuclear quadrupole moment (in nonmagnetic crystals) interacts with the electric-field gradient (EFG) at the probe nucleus. This interaction causes the nucleus to reorient and to emit the second γ-ray into a different region of space than where it would have emitted the second γ-ray if no interaction had occurred. This measurable effect is the basis for PAC spectroscopy. Specifically, two tractable probes are $^{181}Hf \rightarrow {}^{181}Ta$ and $^{111}In \rightarrow {}^{111}Cd$, which both have spin I = 5/2 intermediate levels and which have intermediate-level half lives of 10.8 nsec and 85 nsec, respectively. To investigate Ti-containing perovskites such as $PbTiO_3$ and $BaTiO_3$, the $^{181}Hf \rightarrow {}^{181}Ta$ probe has the appropriate chemistry to substitute into the Ti sites. However, for this probe the ^{181}Ta nucleus undergoes the actual hyperfine interaction with the extranuclear environment.

Measurements of static probe-site EFGs yield sharp spectral lines when each probe nucleus in the ensemble interacts with an identical EFG. This situation occurs when the probes occupy a specific site in a nearly perfect crystal. The measurements yield broadened lines when point defects lie close to the probe site and each probe in the ensemble interacts with a somewhat different EFG. When this situation occurs, a distribution of EFGs characterizes the interaction. However, even an infinitely-broad distribution of static EFGs does not completely destroy the angular correlation. In contrast to static EFGs, the measurement of EFGs that fluctuate on the PAC experimental time scale, which, for the $^{181}Hf \rightarrow {}^{181}Ta$ probe, varies from ≈ 0.1 to 80 nsec, yields spectral lines that show increasing attenuation as the intermediate-level lifetime increases. An interaction with a fluctuating EFG eventually causes the destruction of the angular correlation because the fluctuations change the direction of the quantization axis; we refer to this process as "nuclear-spin relaxation".

PAC spectroscopy has been used to investigate both magnetically-ordered and electrically-ordered pervoskites. The investigations of magnetic crystals using non-magnetic probes primarily have involved measuring supertransferred hyperfine fields at the nuclear probe sites via the magnetic-dipole interaction [13, 14]. These fields arise when electron-spin density is transferred through ligand p orbitals to 4s and 5s orbitals of the probe ion, which is a non-magnetic impurity ion that occupies a metal-ion crystal site. These fields provide unique information about the spatial extents of atomic wave functions in the crystal [14]. The investigation of ferroelectric and antiferroelectric crystals has involved measuring EFGs at probe sites via the nuclear quadrupole interaction (NQI) [15].

Before the mid-1980's, a variety of ferroelectric and antiferroelectric titanates, zirconates, and hafnates had been investigated using PAC spectroscopy, which had involved using primarily the $^{181}Hf \rightarrow {}^{181}Ta$ probe, although the $^{44}Ti \rightarrow {}^{44}Sc$ and $^{111}In \rightarrow {}^{111}Cd$ probes had also been used [15]. From these investigations, the relationships had been developed between the crystal structure and the parameters that characterize the measured hyperfine interaction, which occurs at a specific crystal site. During this era, Yeshurun, Schlesinger, and Havlin [16] performed the most detailed investigation on $PbHfO_3$, in which they measured and analyzed critical phenomena associated with two antiferroelectric transitions. This work established that PAC spectroscopy can be used to characterize critical phenomena associated with ferroelectric and antiferroelectric transitions.

To use PAC spectroscopy to measure critical effects that are associated with ferroelectric and antiferroelectric transitions has been a difficult undertaking. In contrast to measuring critical effects that accompany magnetic transitions, the effects, as they are manifest in the PAC measurements, are difficult

to discern, and the interpretation of the measurements is even less clear. Using PAC spectroscopy to measure the critical exponent β has been well established for magnetic transitions in metallic crystals and simple binary compounds [17]. In this application, the magnetic hyperfine field (MHF) at the probe site is measured; and, for the cases of interest, it is proportional to the bulk-crystal magnetization, which is the order parameter for the transition. Thus, the analysis of the dependence of the MHF on the reduced temperature, at temperatures that are very close to the critical temperature T_c, can provide the critical exponent β. In addition, these critical exponents, which are derived from PAC measurements on metallic ferromagnets, appear to be independent of the chemical identity of the probe atom [18]. Thus, in the case of ferromagnetic transitions the coupling of the order parameter to the PAC-measured quantity, the MHF, is clearly defined.

In contradistinction, the case of the electrically-ordered perovskites is much more complex. To exhibit ferroelectricity, the crystal must have a low symmetry, which often generates asymmetric EFGs at the metal-ion sites. But metal-ion-site EFGs characterize *non-ferroelectric* low-symmetry crystals also [19]. Thus, the EFG is not a singular property that electric ordering produces. The EFG arises from distortion of the crystal lattice that may be accompanied by electric ordering. Therefore, features of the PAC measurements that characterize the electrical ordering during a transition may be difficult to discern from features that characterize the associated change in crystal structure. In addition, many perovskites that undergo a transition from a ferroelectric to a paraelectric phase show non-vanishing metal-ion-site EFGs in the paraelectric, cubic phase [15, 20]. When the paraelectric phase has cubic symmetry, e. g., the high-temperature phases of $PbTiO_3$ and $BaTiO_3$, the corresponding EFG should vanish. Instead, very weak, temperature independent EFGs are observed, which are thought to arise from the presence of static point defects that lie in the vicinity of the probe ions [20]. This feature makes accurately measuring the EFG temperature dependence at temperatures very close to T_c very difficult.

These aspects of the ferroelecric perovskites may limit the information that one can ultimately derive from PAC measurements on bulk ceramic samples of these important materials. Relatively few investigations using PAC spectroscopy have been performed [15] to characterize the phase transitions that ferroelectric and other perovskites undergo. This statement characterizes the situation when we began investigating these materials during the late 1980's. Aside from several of the initial investigations that we have reported [15, 19, 20], this situation still persists. The compounds $PbTiO_3$ and $BaTiO_3$ are well suited for a PAC investigation, because the $^{181}Hf \rightarrow {}^{181}Ta$ probe substitutes into the Ti sites. Both compounds exhibit ferroelectric (tetragonal)-to-paraelectric (cubic) transitions, at 700 K and 403 K respectively, which traditionally have been viewed as displacive, first-order transitions [1]. Although the transition in $PbTiO_3$ continues to be viewed as this type, more recently, for $BaTiO_3$ some x-ray diffraction [3], Raman scattering [21], and impulsive-stimulated Raman scattering [5] measurements indicate that this nominally first-order transition shows evidence for an order-disorder mechanism [3, 5, 21]. Thus, $PbTiO_3$ provides a paradigm of a strongly first-order displacive transition; whereas, $BaTiO_3$ provides an example of a transition that may show features that characterize first-order and continuous types of transitions.

Therefore, the general question that we pose in this report is: What types of information can be obtained from PAC measurements performed on ceramic perovskites? The answer that we provide is, however, not general, but it provides limited information about the high-temperature transitions that the two ferroelectric perovskites, $PbTiO_3$ and $BaTiO_3$ undergo. These answers may stimulate both further experimental and new theoretical investigations of perovskite crystals.

II. Experimental Details

Samples of $PbTiO_3$ and $BaTiO_3$ were prepared using a resin-intermediate process. To a solution of ethylene glycol and citric acid, the titanium precursor $Ti(OC_3H_7)_4$ and either $Ba(OOCH_3)_2$ or $Pb(OOCCH_3)_2$ were added. The ^{181}Hf activity was carried by a dilute aqueous solution of $HfOCl_2$, and it was added to the $PbTiO_3$ preparation at ≈ 0.25 at.% of the Ti concentration and to the $BaTiO_3$ preparation at ≈ 0.08 at.% of the Ti concentration. The resin was formed by heating the solution that contained the chelated metal ions. The resin was subsequently pyrolyzed and then calcined at 1070 K. As indicated by x-ray powder diffraction, the $PbTiO_3$ compound formed during the calcination, and it received no further processing. The calcined powder for the $BaTiO_3$

preparation was pressed into small pellets and sintered in air at ≈ 1800 K for about an hour. The x-ray powder diffraction patterns were measured on small amounts of powder taken from the radioactive samples on which the PAC measurements were made, and the samples were found to be phase pure to within several percent.

Recent reviews present most of the experimental details involved with performing and analyzing the PAC experiments [8, 22].The experimental time distributions were measured using a four - BaF_2 - detector PAC spectrometer which has a time resolution of ≈ 800 psec full width at half maximum. A specially-designed furnace and temperature control system was used to maintain the samples at constant temperature, ± 0.03 K, during the measurement periods of 0.5 - 1 day. Also the controller was adjusted to avoid significant overshoots and undershoots when the sample temperature was either increased or decreased. We note that the $BaTiO_3$ measurements were performed using the first-design furnace that was large in diameter. The source-to-detector distances were ≈ 9 cm, which required using relatively strong sources. The resulting measurements included prompt coincidences that destroyed the first 1 - 2 nsec regions of the time distributions. The $PbTiO_3$ measurements were performed using a second-generation furnace that is smaller in diameter. The corresponding source-to-detector distances are ≈ 5 cm, which reduces the effects of prompt coincidences. The perturbation functions $A_{22}G_{22}(t)$ were determined from the time distributions. A two-site model for static nuclear-electric-quadrupole interactions was sufficient to analyze the measured perturbation functions:

$$-A_{22}G_{22}(t) = \sum_{j=1}^{2} A_j \left[S_0 + \sum_{k=1}^{3} S_k \exp(-\delta_j \omega_{jk} t) \cdot \cos(\omega_{jk} t) \right] + A_3. \quad (1)$$

Here A_1 and A_2 are the normalization factors, δ_1 and δ_2 are the line-shape parameters, which represent the relative widths of the Lorentzian frequency distributions (of the corresponding frequency sets) that give rise to static linebroadening; and A_3 takes into account the effects of γ-rays that are absorbed by the sample en route to the detectors, which were small in these experiments, and the effects of probes that reside in non-perturbed environments. The site-occupancy fractions are represented by $f_i = A_i/(A_1 + A_2 + A_3)$, $i = 1, 2$. For each probe site (each phase), the frequencies ω_k and the corresponding amplitudes $S_k(\eta)$ describe a static interaction in a polycrystalline source, and the ratio ω_2/ω_1 is used to determine the associated quadrupole frequency ω_Q and asymmetry parameter η. The nonvanishing EFG components V_{ii} in the principal-axis system where the probe nucleus is at the origin are related to the quadrupole frequency and asymmetry parameter by $\omega_Q = eQV_{zz}/4I(2I-l)\hbar$ and $\eta = (V_{xx} - V_{yy})/V_{zz}$ in which Q represents the nuclear electric-quadrupole moment (2.51 b) for the ^{181}Ta spin $I = 5/2$ intermediate level.

III. Results and Discussion

Figure 1 presents several perturbation functions for $PbTiO_3$ that were measured at temperatures very close to T_c and that illustrate the effects of the tetragonal-to-cubic transition on the Ti-site EFG. The perturbation functions measured above $T_c \approx 760.5 \pm 0.5$ K show little structure and represent very weak perturbations. Perturbation functions measured at temperatures several hundred degrees higher show the same shape. Thus, above T_c, the Ti-site EFG becomes temperature independent. To fit the above $-T_c$ perturbation functions, we used (1) and constrained the frequencies so that $\eta \approx 0$. Typically, the fits required using admixtures in the fitting function of a very-low-frequency, highly-damped static-interaction term and a zero-frequency term (A_3 in (1)). These conditions strongly suggest that point defects, which give rise to weak static interactions, occupy positions near some of the probes and the remainder of probes occupy defect-free environments, which give rise to no interactions.

The perturbation functions measured below T_c show the features of at least two interactions, a relatively strong well-defined interaction that increases in strength only slightly as temperature decreases from T_c, and a very weak interaction. To fit the below $-T_c$ perturbation functions, we used (1) and constrained the frequencies so that $\eta = 0$. Typically, the fits required using, in the fitting function, two static-interaction terms and a zero-frequency term. The term that represented the strong well-defined interaction yielded unique parameters that vary systematically with temperature changes and gave $V_{zz} \approx 4 - 5 \times 10^{17}$ Vcm^{-2} and $\delta \approx 0.15 \pm 0.05$. The term that represented the very weak interaction along with the zero-frequency term yielded parameters that were

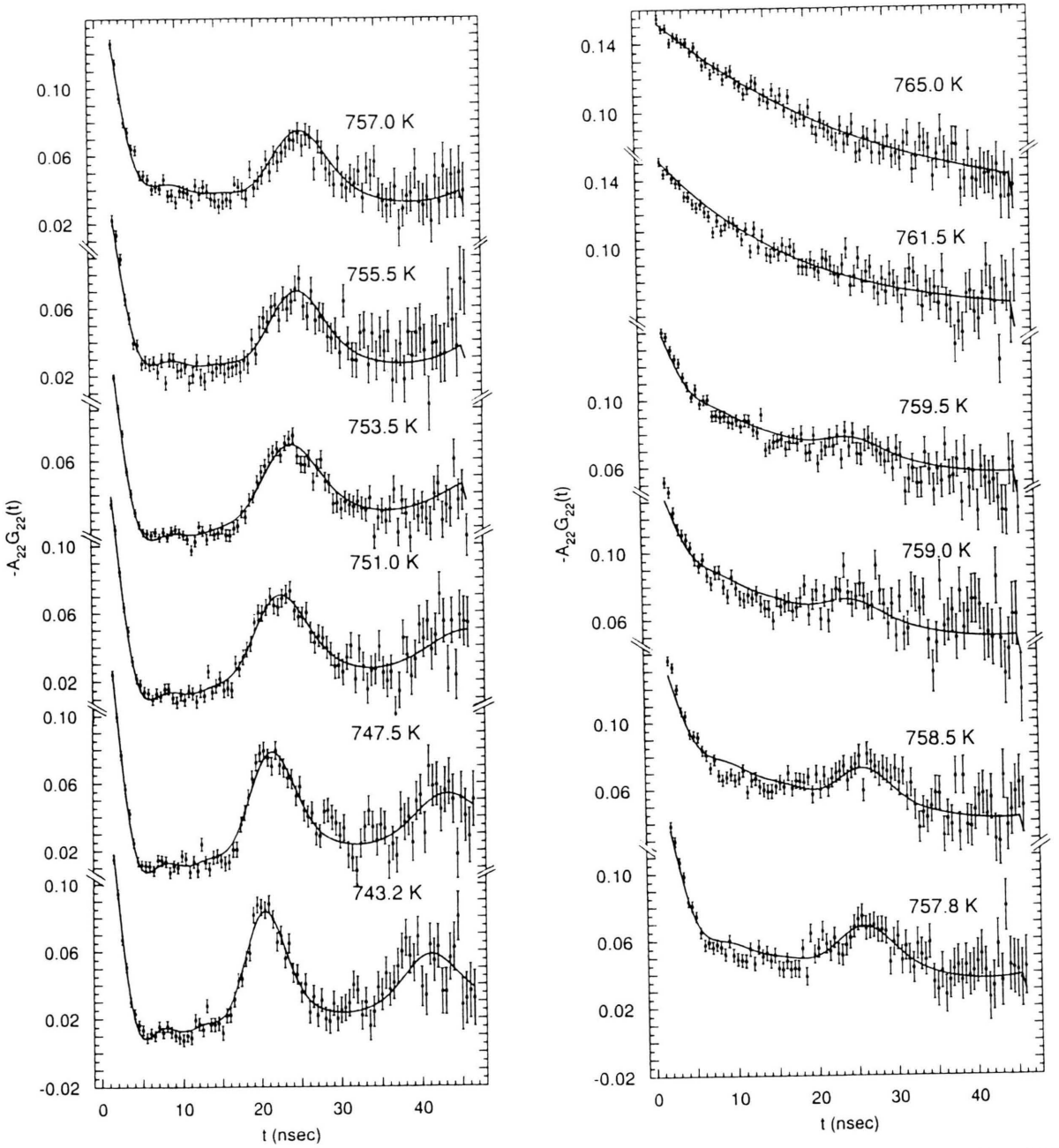

Fig. 1. Perturbation functions for a $PbTiO_3$ powder sample at increasing temperatures. The solid lines represent fits of (1) to the data points. For this set, $T_c = 760.5 \pm 0.5$ K. The two functions measured at 761.5 K and 765.0 K represent the paraelectric phase, which has nominal cubic symmetry but nonvanishing EFGs.

difficult to characterize. At temperatures very close to T_c (that correspond, for example, to some of the perturbation functions shown on the right side of Figure 1), this component gave $V_{zz} \approx 0.1 \times 10^{17}$ Vcm^{-2} and $\delta \gg 1$; and, at temperatures further away from T_c (that correspond to the perturbation functions shown on the left side of Fig. 1), this component gave $V_{zz} \approx 1 \times 10^{17}$ Vcm^{-2} and $\delta < 1$. Generally, acceptable fits

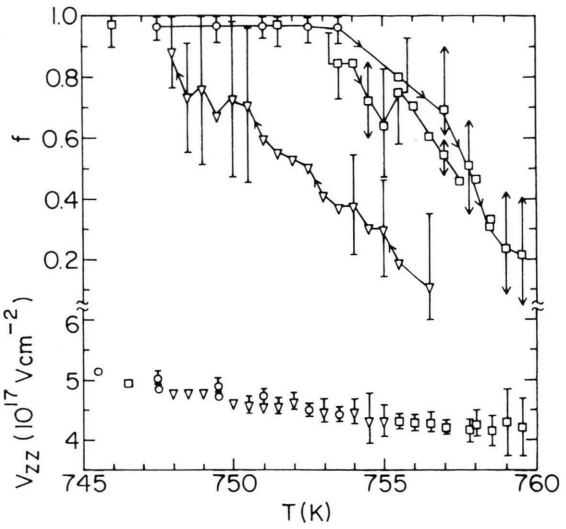

Fig. 2. Parameter summary for the analysis of the measurements on a $PbTiO_3$ powder sample. The V_{zz}-values correspond to the high-frequency interaction that occurs below T_c, and the f-values represent the corresponding fractions of probes that underwent this interaction. The circles represent fits that consist of a single static-interaction term plus a zero-frequency term in (1). The squares (T increasing) and the triangles (T decreasing) represent fits that consist of two static-interaction terms plus a zero-frequency term.

could not be obtained with $A_3 = 0$. Thus, we associate the strong well-defined interaction with the tetragonal, ferroelectric phase, because the corresponding EFG parameters resemble those that characterize the Ti-site interaction at temperatures well below T_c, in which V_{zz} is large, η is near zero, and δ is moderate (at laboratory temperature, $V_{zz} = 14.5 \pm 0.1 \times 10^{17}$ Vcm^{-2}, $\eta = 0.02 \pm 0.02$, and $\delta = 0.04 \pm 0.01$). The other interaction cannot be accurately characterized over the ≈ 8 K range where multiple Ti-site interactions take place, and it does not completely resemble the interaction observed above T_c. Therefore, we speculate that complex physical changes could occur in sample regions where the probes appear to undergo this poorly-defined interaction; and the static model (1), which includes no spin-relaxation effects, does not provide a good representation of these effects.

Figure 2 presents a summary of the V_{zz} and site-occupancy fraction f values that represent the aforementioned strong, well-defined interaction. The values of the EFG component V_{zz} change by less than 20 % over the indicated 15 K interval, and these values do not depend on whether the measurements involved either successive increases or successive decreases

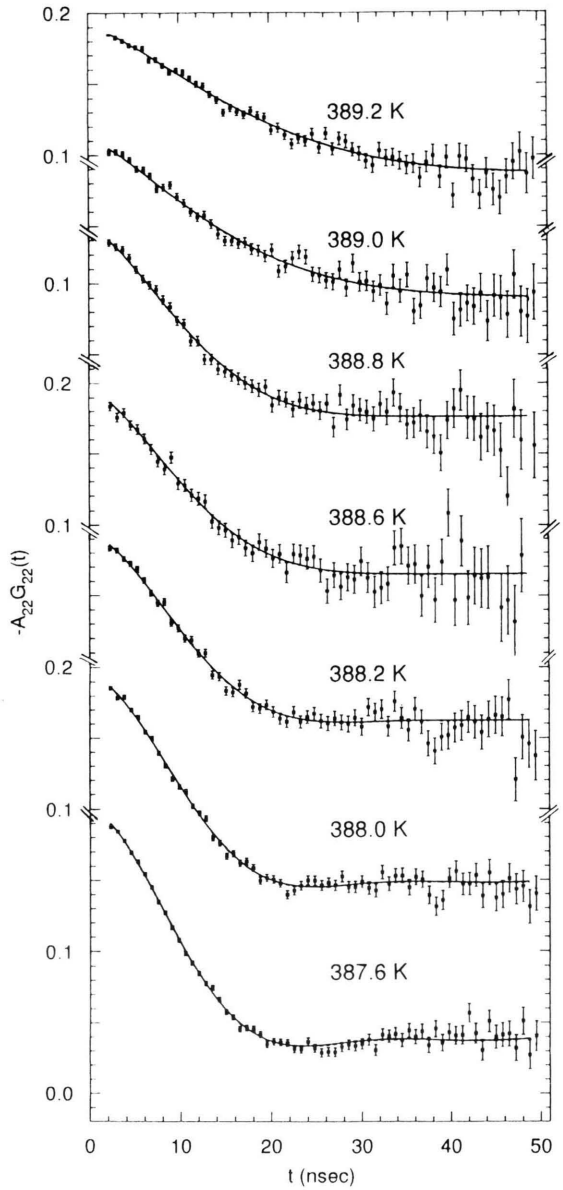

Fig. 3. Perturbation functions at various temperatures for a sintered-ceramic sample of $BaTiO_3$. Solid lines: fits of (1) to the data points. For this set, $T_c = 390.3 \pm 0.4$ K. The function at 389.2 K is typical for the paraelectric phase, in which the EFGs do not vanish.

of the temperature. The site-occupancy values show clear evidence for the onset of the tetragonal-to-cubic transition. Therefore, we associate the measurement of these two interactions with the coexistence of the tetragonal and cubic phases within the sample. The f-values change from one to zero over an 8 ± 1 K range. However, these f-values can only be accurately

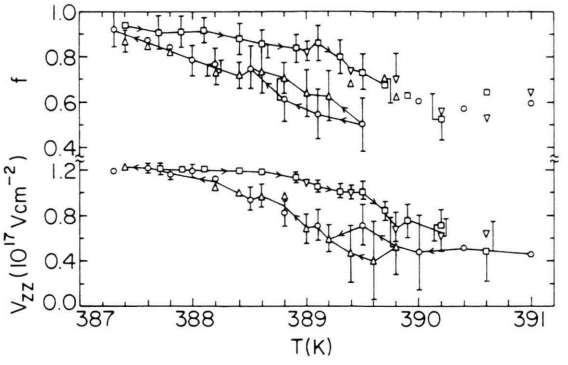

Fig. 4. Parameter summary for the analysis of the measurements on a $BaTiO_3$ ceramic sample. For the V_{zz}- and f-values measured at increasing temperatures, T_c = 390.3 ± 0.4 K, and for those measured at decreasing temperatures, T_c = 389.2 ± 0.4 K, the fits represent the sum of a static-interaction term and a zero-frequency term.

measured over the range $\approx 0.2 \leq f \leq \approx 0.8$. The locus of f-values that corresponds to measurements performed at successively higher temperatures is displaced by 5 ± 1 K from the locus that corresponds to measurements performed at successively lower temperatures. This difference indicates that considerable thermal hysteresis accompanies this transition. The error bars indicated on the f-values appear to be very large. These error bars are determined using standard non-linear regression analysis. As such, they represent confidence intervals that reflect the uniqueness of the derived parameters. Because non-unique-parameters describe one of the two interactions that the f-values represent, these error bars tend to appear to be large. Nonetheless the f-values are not indeterminate. They vary systematically and appear to be self-consistent.

Figure 3 presents several perturbation functions for $BaTiO_3$ that were measured at successively decreasing temperatures very close to T_c and that illustrate the effects of the tetragonal-to-cubic transition on the Ti-site EFG. The 389.2 K perturbation function is representative of those measured just above T_c as well as those measured several hundred degrees higher. Those measured at successively-lower temperatures below T_c show increasingly-stronger perturbations. To fit these perturbation functions, we used (1) and constrained the frequencies so that $\eta = 0$. Generally, acceptable fits either for the below – or for the above $-T_c$ measurements could not be obtained with $A_3 = 0$. Values of $V_{zz} \approx 0.5 \pm 0.2 \times 10^{17}$ Vcm^{-2}, $\delta \approx 0.5 \pm 0.2$, and $f \approx 0.5 \pm 0.1$ characterize the above $-T_c$ interactions; and, below T_c, V_{zz} ranges from ≈ 0.5 - 1.2×10^{17} Vcm^{-2} over an interval of roughly 4 K. Figure 4 summarizes the temperature dependences of the V_{zz}- and f-values.

This information strongly suggests that two probe environments characterize the Ti-sites in the cubic phase: one corresponds to a Ti-site around which some point defects are located, and one corresponds to a defect-free environment where the EFG vanishes. At temperatures near-but-below T_c, EFGs produced by the tetragonal lattice distortion and EFGs produced by point defects are comparable in magnitude, and their effects are difficult to separate in the measurements. In this temperature region, the site-occupancy fractions represent the fractions of probes that are not located in purely zero-frequency environments. The corresponding V_{zz} values include contributions produced by point defects, which persist at temperatures above T_c, and contributions from the lattice distortions. Since these two effects are not strictly additive, the effects of the defect-produced EFG contribution cannot be removed by direct subtraction of the above $-T_c$ measured average V_{zz} value. At temperatures $\approx$ 1 - 2 K or more below T_c, the weak defect-produced EFG becomes insignificant, and the V_{zz} values reflect the effects of the lattice distortion and ferroelectricity. Thus, the non-vanishing, above $-T_c$ EFG contribution limits the information that we can derive from EFG measurements performed at temperatures very close to but below T_c.

Discussion

A large amount of experimental information [3, 5, 21] indicates that the tetragonal-to-cubic transition in $BaTiO_3$ has order-disorder features. If this transition were strictly first-order in character, we would not expect to observe evidence for critical effects. Because the transition does show order-disorder features that can be associated with continuous transitions, we, therefore, might expect the transition to show evidence for critical effects. The power-law dependence of a quantity proportional to the order parameter for the transition would constitute this type of evidence, and the corresponding exponent would represent the critical exponent β [23]. For the ferroelectric-to-paraelectric transition, the electrical polarization of the crystal represents the order parameter [1, 23]

We posit the hypothesis that the EFG component V_{zz} is proportional to the order parameter, which is the

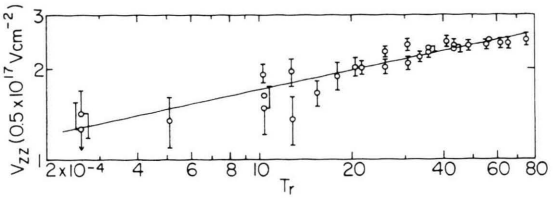

Fig. 5. The power-law dependence for $BaTiO_3$ of V_{zz}, measured very close to T_c, on the reduced temperature T_r. The reduced temperatures were calculated separately for the V_{zz} values measured at increasing and decreasing temperatures.

electrical polarization of the crystal. To test the hypothesis, first we determine the T_c values from the V_{zz} temperature dependences; one T_c-value corresponds to the temperature-increasing series of measurements and one corresponds to the temperature-decreasing series. Second, we calculate the reduced temperature values $T_r = 1 - (T/T_c)$ for each set of measurements and plot both sets of (T_r, V_{zz}) data points on logarithmic coordinates. Figure 5 represents this analysis, and the derived power-law exponent is 0.21 ± 0.05. We determined the apparent uncertainty in this value by using limiting slopes. In addition, the choice of T_c values produces a non-explicit uncertainty that has approximately the same magnitude. Despite these sizable uncertainties, the dependence of log V_{zz} on log T_r shows a strong linear correlation, which we also observed in several earlier sets of measurements [24, 25]. The derived β-value is lower than the values that we would expect to observe during a transition in a three-dimensional crystal, $0.3 \leq \beta \leq 0.4$ [23]. However, the V_{zz} values measured above T_c represent, we believe, the EFGs generated by static point defects; and, therefore, the V_{zz} values just below T_c represent both the EFGs generated by the ferroelectric lattice distortion and the EFGs generated by the point defects. At these temperatures, the defect contribution to the total values is significant. Therefore, a correction should be made to the below $-T_c$ V_{zz} values for the EFGs generated by the defects. Calculating the average above $-T_c$ V_{zz} value and subtracting it from each of the below $-T_c$ values would produce too large of a correction, and V_{zz} would decrease too rapidly, i. e., β would become too large. Performing no correction causes V_{zz} to decrease too slowly as T_r decreases, and β would become too small. We know from previous experience [24, 25] that subtracting a V_{zz}-value of one-half of the average above $-T_c$ V_{zz} value would give $\beta \approx 0.3$, which would be a reasonable value. Therefore, the power-law dependence of V_{zz} on T_r

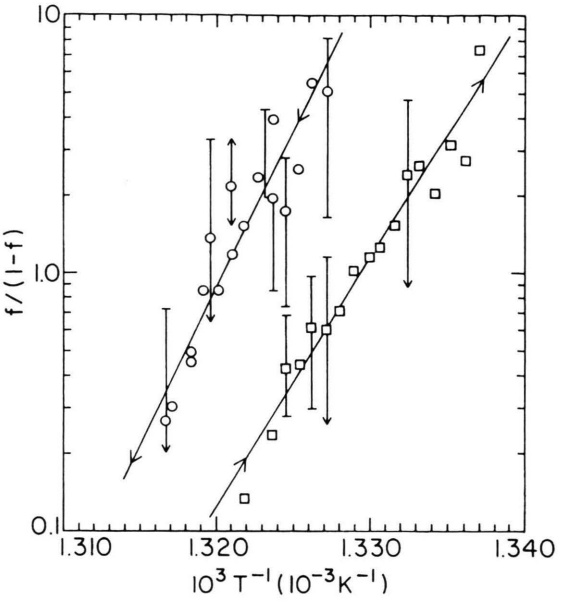

Fig. 6. Dependence of the logarithm of $f/(1\text{-}f)$ on the inverse temperature for $PbTiO_3$, $f/(1\text{-}f)$ representing the number of probes undergoing the tetragonal-phase interaction divided by the number of probes undergoing other interactions. The solid lines represent least-squares fits. The energies derived from the slopes are 23.7 ± 5 eV for the increasing temperatures and 18.7 ± 4 eV for the decreasing temperatures.

shows the qualitative features that we expect critical effects in $BaTiO_3$ to exhibit. But we need to develop a model that would provide a means to separate the contribution of defect-generated EFGs to the below-but-near-T_c V_{zz}-values.

Because the tetragonal-to-cubic transitions for both $PbTiO_3$ and $BaTiO_3$ have been identified traditionally as being first-order transitions [1], we must consider the physical significance of the corresponding site-occupancy-fraction temperature dependences. If these transitions were truly first-order, then we would expect the two phases, which are the tetragonal and cubic phases in this case, to coexist only at a specific temperature T_c. We examine these temperature dependences, which Figs. 2 and 4 show respectively for $PbTiO_3$ and $BaTiO_3$, and we observe that the two phases coexist over relatively broad intervals of ≈ 8 K and ≈ 2 K, respectively. This observation is not consistent with the character of first-order transitions. However, these transitions show thermal hystereses of ≈ 4 K and ≈ 1 K, respectively, which do characterize first-order transitions.

To further analyze the site-occupancy information, we form the ratio, $f/(1-f)$, that represents the ratio

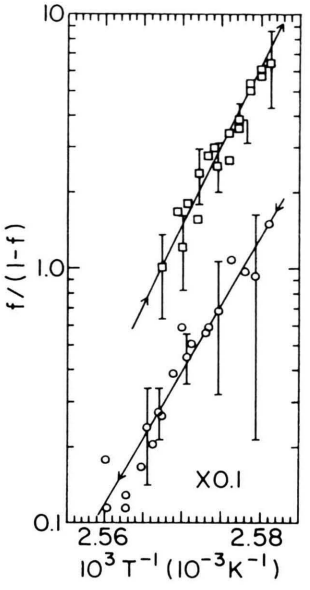

Fig. 7. Dependence of the logarithm of $f/(1\text{-}f)$ (cf. Fig. 6) on the inverse temperature for $BaTiO_3$. The solid lines represent least-squares fits. The energies are 10.4 ± 3 eV for the increasing temperatures and 12.5 ± 3 eV for the decreasing temperatures.

of the probe concentration in the tetragonal phase to the probe concentration in the cubic phase (more accurately, the probe concentration in all other environments). This ratio shows a reasonably strong linear correlation with inverse temperature. Figures 6 and 7 show this dependence for $PbTiO_3$ and $BaTiO_3$, respectively. We observe that the slopes of the lines are rather large, since the inverse temperature scale spans only several degrees. The slopes that correspond to the values measured at successively higher temperatures are approximately equal to the slopes that correspond to the values measured at successively lower temperatures. Although graphs of this type are commonly refered to as "Arrhenius plots", several physical interpretations of the slope of the line may be invoked. One interpretation involves the kinetics of a process. When the logarithm of a quantity proportional to the rate of a process is plotted as a function of inverse temperature, the analysis of the slope gives the activation energy ΔE, which represents the height of a kinetic barrier. A very different interpretation arises when the process is at chemical equilibrium. Under this condition, when the logarithm of the equilibrium constant K is plotted as a function of inverse temperature, the analysis of the slope gives the standard-state Gibbs free-energy change for the process ΔG°, which represents the free-energy required to convert a specific quantity of reactants into products.

For $PbTiO_3$ and $BaTiO_3$, the average slopes of the lines shown in Figs. 5 and 6 give energies of 21 ± 5 eV and 11 ± 3 eV, respectively. These energies are much too large to represent either activation energies or Gibbs free-energies. Therefore, the Arrhenius-type plots, which Figs. 6 and 7 show, represent a convenient way to linearize the probe-concentration ratios that characterizes these transitions, but they do not yield energies that describe any known physical process in crystals. To analyze the probe-concentration ratios, which represent the coexistence of both phases at the corresponding temperatures, we attribute the origin of this coexistence of two phases to the effects of a distribution of T_c-values within the sample. According to this hypothesis, the actual transition temperature would vary throughout the crystal. At any specific temperature within a temperature interval that is very close to T_c, the temperature in some regions of the crystal would exceed T_c; and, in other regions, the temperature would not exceed T_c. Thus, we would observe a different probe-concentration ratio at each temperature within the interval. Our colleagues at Brigham Young University [26] have proposed this hypothesis, and they have developed a specific model that gives the transition temperatures a Gaussian distribution, which has a mean transition temperature T_c and a standard deviation σ. Using this model, the fraction of probes that undergo the above $-T_c$ interaction at temperature T is given by the fraction of transition temperatures $F(T)$ that occur in the temperature interval: $-\infty \leq T' \leq T$, in which T' is the random variable, namely the local transition temperature. The cumulative distribution function gives the site-occupancy fraction

$$f = 1 - F(T) = \frac{1}{2}\left[1 + \mathrm{erf}\left[(T - T_c)/\sqrt{2}\cdot\sigma\right]\right]. \quad (2)$$

If we consider values of T that are close to T_c, which is a physically realistic situation, then the expression for the probe-concentration ratio becomes

$$\ln(f/(1-f)) = -\frac{2\sqrt{2}}{\sqrt{\pi}\sigma}T_c + \frac{2\sqrt{2}k}{\sqrt{\pi}\sigma kT}T_c^2, \quad (3)$$

in which k represents the Boltzmann constant. We recognize that the apparent energies, either ΔE or ΔG°,

when divided by k, are equal to $2\sqrt{2}T_c^2/\sqrt{\pi}\sigma$; and the corresponding standard deviations are equal to 3 ± 1 K for $PbTiO_3$ and 2 ± 1 K for $BaTiO_3$.

This model gives estimates of the variation in the transition temperature throughout the sample. The more important question is what effect gives rise to the variation in the local T_c-values, which we appear to observe. We offer the following explanation. The transition takes place when nucleation and growth occur at nucleation sites. If the nucleation sites were in fact uniformly distributed throughout the sample, then we would expect to observe no variation in the transition temperature. If, however, the nucleation sites were actually species that would be present in low concentrations such as point defects, then the local concentrations of these nucleation sites would be inhomogeneous. Because the nucleation sites would be present in relatively small numbers, their corresponding spatial (not temporal) distributions would be subject to statistical fluctuations. Therefore, the local transition temperatures would depend on the local nucleation-site concentration. Variations in the local transition temperature would give rise to the apparent coexistence of both phases that we observe in the sample. In addition to the site-occupancy measurements, which provide direct evidence for the apparent coexistence phenomenon, the above $-T_c$ perturbation functions for both $PbTiO_3$ and $BaTiO_3$ show related evidence. Specifically, these perturbation functions represent two types of probe environments, because accurate fits could only be obtained when a zero-frequency term is included with a static-interaction term in the fitting function. Therefore, above $-T_c$, some probes undergo very weak interactions that nearby defects produce, and some probes undergo no interactions, which indicate the absence of nearby defects. This observation indicates that the point-defect concentrations are not uniform. If these defects were the nucleation sites, then they would give rise to local differences in the transition temperature, and the defects would be responsible for major aspects of the character of these transitions.

IV. Conclusions

We have measured the temperature dependences of the Ti-site EFGs in samples of $PbTiO_3$ and $BaTiO_3$ during the tetragonal-to-cubic transitions. For both compounds, the high-temperature paraelectric phases show very-weak, non-vanishing, temperature-independent Ti-site EFGs. At temperatures very near but below T_c, for $PbTiO_3$, we can separate the EFG produced by the tetragonal crystal distortion associated with the ferroelectric phase from EFGs associated with the paraelectric phase. For $BaTiO_3$, at temperatures very close to T_c, we cannot completely separate the effects produced by the ferroelectric distortion from those associated with the paraelectric phase. This limitation prevents us from deriving accurate values of the critical exponent β from the power-law dependence of V_{zz} on T_r. Despite this limitation, the linear correlation of $\log V_{zz}$ with $\log T_r$ may be evidence for the occurence of critical fluctuations during this nominally-first-order transition. The transitions for both $PbTiO_3$ and $BaTiO_3$ show some thermal hysteresis, which is expected to occur during these first-order transitions, but both compounds also show the coexistence of both phases over a short but significant temperature interval, which is not expected to occur during strictly first-order transitions. Associated with this coexistence phenomenon is an apparent linear dependence of the logarithm of the site-concentration ratio $f/(1-f)$ on inverse temperature. We are able to explain this strong correlation using a model that associates a distribution of transition temperatures T_c with each transition. We attribute the presence of the T_c distributions to inhomogeneous distributions of nucleation sites in the samples, which could be point defects. These results indicate that further experimental and theoretical investigation of phase transitions in perovskite crystals should be carried out.

Acknowledgements

We greatly appreciate the insight into these complex measurements and the wisdom that Professor William E. Evenson and Professor David Allred of Brigham Young University have provided. Their timely development of the T_c-distribution model enabled us to develop a consistent explanation of a rather vexing aspect of this experiment. We thank Professor Darrell G. Schlom of The Pennsylvania State University and Professor Robert L. Rasera of University of Maryland Baltimore County, who contributed much knowledge and expertise. We thank Professor Tilman Butz of Universität Leipzig for his comments and careful review of the manuscript. We thank the Office of Naval Research for partial support via Grant No. N0014-90-J-4112.

[1] See, for example, M. E. Lines and A. M. Glass, Principles and Applications of Ferroelectric and Related Materials, (Clarendon Press, Oxford, 1977), 680pp.
[2] C. H. Perry, R. Currat, H. Buhay, R. M. Migoni, W. G. Stirling, and J. D. Axe, Phys. Rev. **B39,** 8666 (1989).
[3] R. Comes, M. Lambert, and A. Guinier, C. R. Acad. Sci. Paris **226,** 959 (1968); R. Comes, M. Lambert, and A. Guinier, Solid State Communication **6,** 715 (1968).
[4] See, for example, G. Burns and B. A. Scott, Phys. Rev. **B7,** 3088 (1973).
[5] T. P. Dougherty, G. P. Wiederrecht, K. A. Nelson, M. H. Garrett, H. P. Jenssen, and C. Warde, Phys. Rev. **B50,** 8996 (1994).
[6] G. L. Catchen and D. M. Spaar, Phys. Rev. **B44,** 12137 (1991).
[7] See, for example, G. L. Catchen, T. M. Rearick, and D. G. Schlom, Phys. Rev. **B49,** 318 (1994).
[8] G. L. Catchen, Materials Research Society Bulletin **20,** 37 (1995).
[9] M. Eibschütz, S. Shtrikman, and D. Treves, Phys. Rev. **156,** 562 (1967).
[10] T. C. Gibb, R. Greatrex, N. N. Greenwood, and P. Kaspi, Chem. Communication **1971,** 319 (1971); and T. C. Gibb, R. Greatrex, N. N. Greenwood, and P. Kaspi, J. Chem. Soc. Dalton Trans. **1973,** 1253 (1973).
[11] V. G. Bhide and M. S. Multani, Phys. Rev. 149, 289 (1966); and V. G. Bhide and M. S. Hegde, Phys. Rev. **B5,** 3488 (1972).
[12] G. L. Catchen, Hyperfine Interactions **88,** 1 (1994).
[13] T. M. Rearick, G. L. Catchen, and J. M. Adams, Phys. Rev. **B48,** 224 (1993).
[14] H. H. Rinneberg and D. A. Shirley, Phys. Rev. Lett. **30,** 1174 (1973).
[15] For a review of the earlier PAC experiments performed on perovskites, see: G. L. Catchen, S. J. Wukitch, E. M. Saylor, W. Huebner, and M. Blaszkiewicz, Ferroelectrics **117,** 175 (1991).
[16] Y. Yeshurun, Y. Schlesinger, and S. Havlin, J. Phys. Chem. Solids **40,** 231 (1979); and Y. Yeshurun, S. Havlin, and Y. Schlesinger, Solid State Communication **27,** 181 (1978).
[17] C. Hohenemser, N. Rosov, and A. Kleinhammes, Hyperfine Interactions **49,** 267 (1989); and references therein.
[18] C. Hohenemser, T. Kachnowski, and T. K. Bergstrasser, Phys. Rev. **B13,** 13154 (1976).
[19] G. L. Catchen, S. J. Wukitch, D. Spaar, and M. Blaszkiewicz, Phys. Rev. **B42,** 1885 (1990).
[20] J. M. Adams and G. L. Catchen, Mat. Sci. and Eng. **B15,** 209 (1992).
[21] J. P. Sokoloff, L. L. Chase, and D. Rytz, Phys. Rev. **B38,** 597 (1988).
[22] G. L. Catchen, J. Materials Education **12,** 253, (1990).
[23] H. B. Callen, Thermodynamics and an Introduction to Thermostatistics (John Wiley and Sons, New York, ed. 2, 1985), pp. 215-276.
[24] G. L. Catchen, T. M. Rearick, E. F. Hollinger, D. W. Esh, and J. M. Adams, Ferroelectrics **156,** 239 (1994).
[25] E. F. Hollinger, Master of Science Thesis, Characterization of the Ferroelectric-to-Paraelectric Phase Transition in Barium Titanate by Perturbed Angular Correlation Spectroscopy, The Pennsylvania State University, 1995.
[26] W. E. Evenson and D. Allred, unpublished research.